Nijenhuis et al., http://www.jcb.org/cgi/content/full/jcb.201210033/DC1

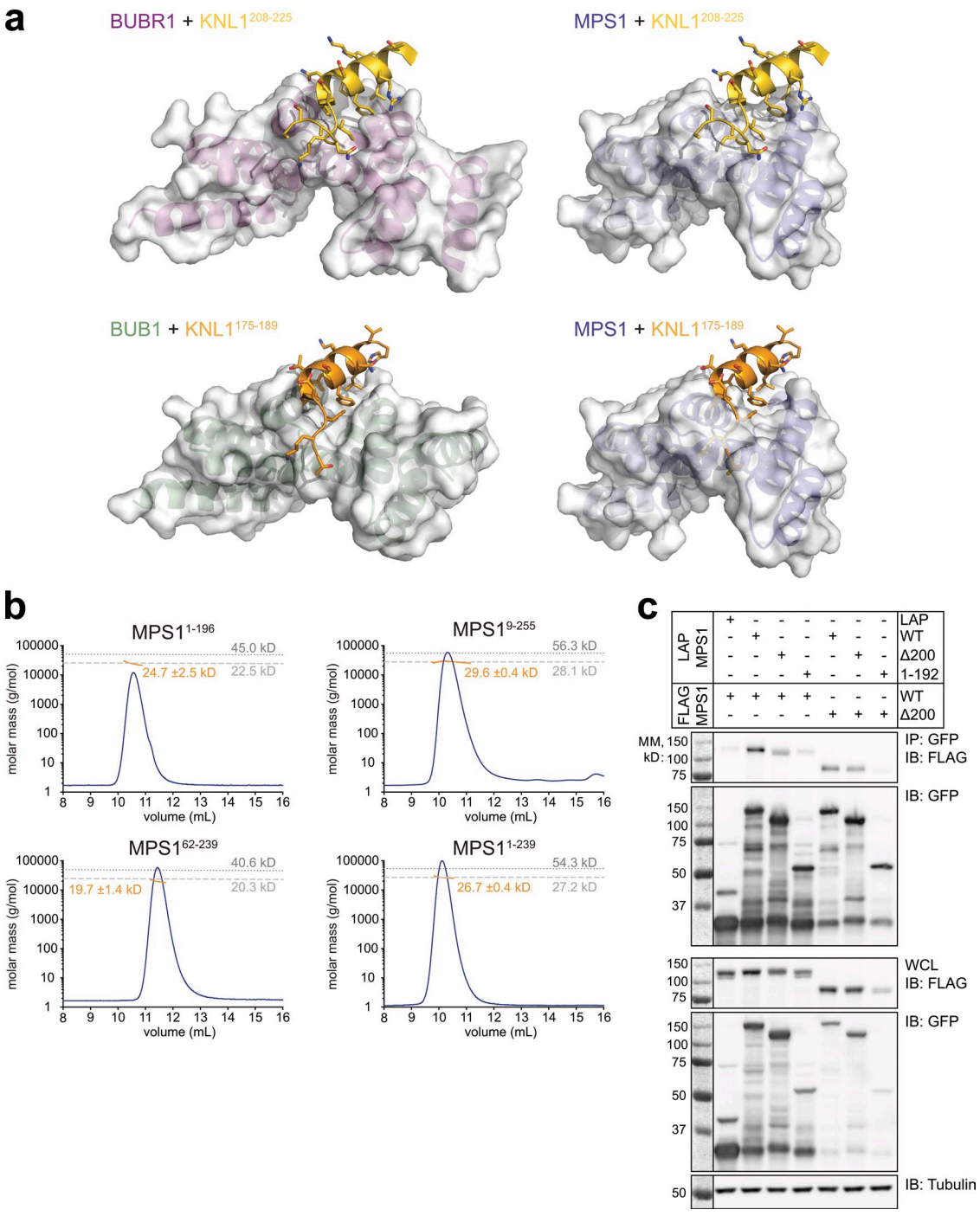

Figure S1. **MPS1 TPR lacks the characteristic KNL1-binding depression of BUB TPR domains and is monomeric in solution.** (a) Crystal structures of the BUB1 (Protein Data Bank accession no. 4A1G) and BUBR1 (Protein Data Bank accession no. 3SI5) TPR domains in complex with a KNL1 peptide and structural superposition-based models of the binding of the MPS1 TPR domain to these peptides. The TPR domains are shown as cartoon diagrams in a semitransparent surface as in Fig. 1 c. The orientation has been chosen to best illustrate the interaction interface with the KNL1 peptide, represented as a cartoon diagram with all side chains shown as sticks. The superposition-based models for MPS1 illustrate the lack of the characteristic surface depression that facilitates KNL1 binding in the BUB TPR domains. (b) Size-exclusion chromatography and multiangle laser light scattering measurements of MPS1$^{1–196}$, MPS1$^{9–255}$, MPS1$^{62–239}$, and MPS1$^{1–239}$. The mean *M*r per volume unit (yellow lines) and the normalized UV_{280nm} elution profile (solid blue lines) are shown. The theoretical *M*r values for the monomeric and dimeric forms are represented as dashed horizontal lines. Graphs representative of at least two experiments. (c) FLAG and GFP immunoblots (IB) of whole-cell lysates (WCL; bottom) or immunopurified (IP) FLAG-MPS1 (wild type [WT] and Δ200; top) from mitotic HEK 293T cells coexpressing FLAG-MPS1 and LAP-MPS1 variants (as indicated). Boxes on left show molecular mass standard. MM, molecular mass.

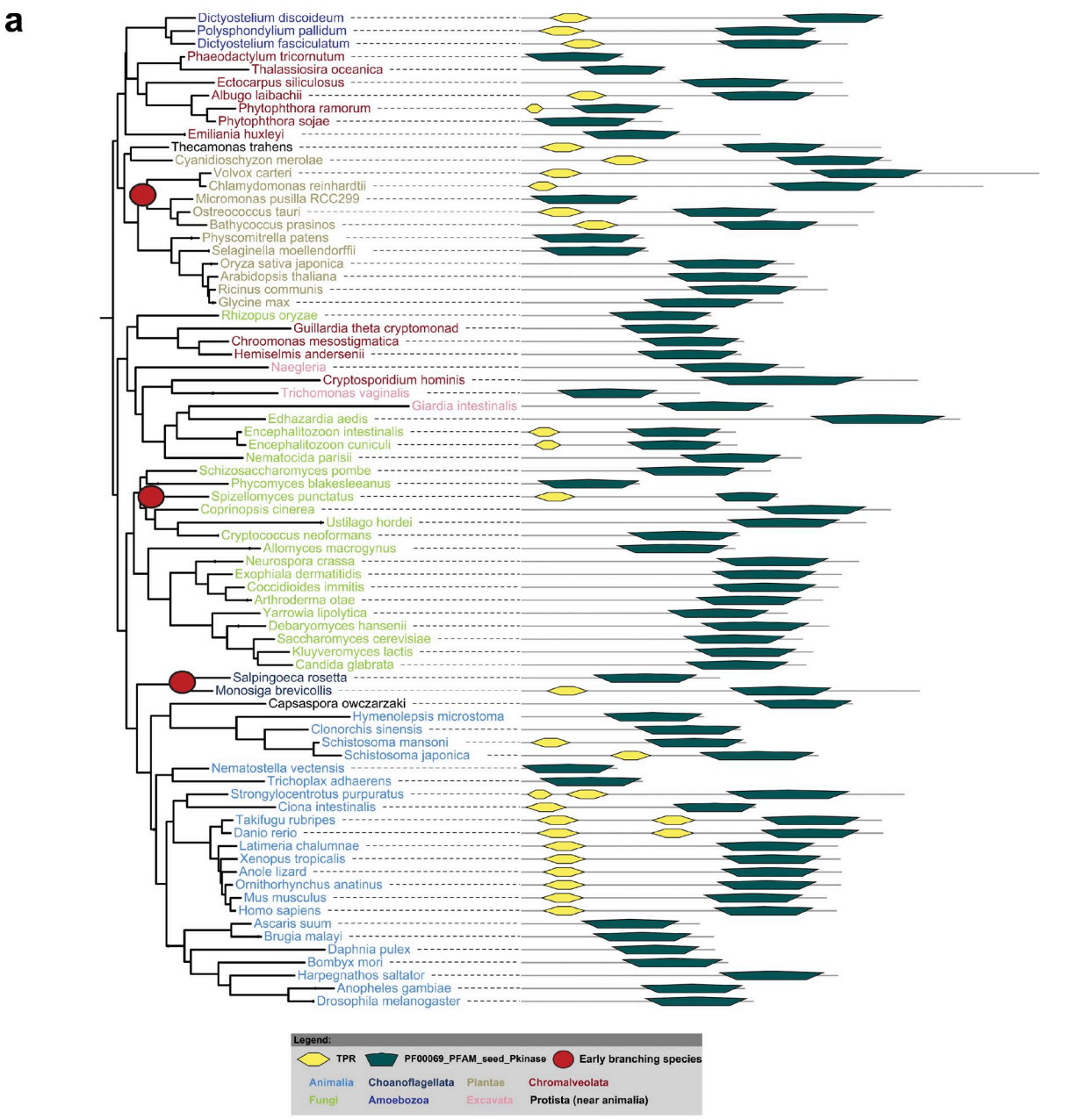

Figure S2. **Phylogenetic analysis of the MPS1 TPR domain.** (a) Phylogenetic tree of MPS1 homologues, based on the kinase domain. Differential coloring of major eukaryotic groups reveals clustering consistent with the eukaryotic species tree. Projection of the MPS1 domain topology onto the homologue tree shows a patchy distribution of the TPR domain, indicative of parallel evolution. Parallel loss is indicated by the presence of the TPR domain in species that branched off early relative to neighboring species in their major groups, e.g., algae versus plants and choanoflagellates versus animals (see red circles). Please note that we cannot formally exclude the possibility that incomplete gene annotation is an occasional reason for our inability to identify TPR domains in certain species (e.g., *Salpingoeca rosetta*, *Nematostella vectensis*, *Trichoplax adhaerens*, and several chromaveolata). (b) Sequence alignment of the TPR domains of MPS1 homologues. Colors represent amino acid characteristics following the generally used Clustal definition.

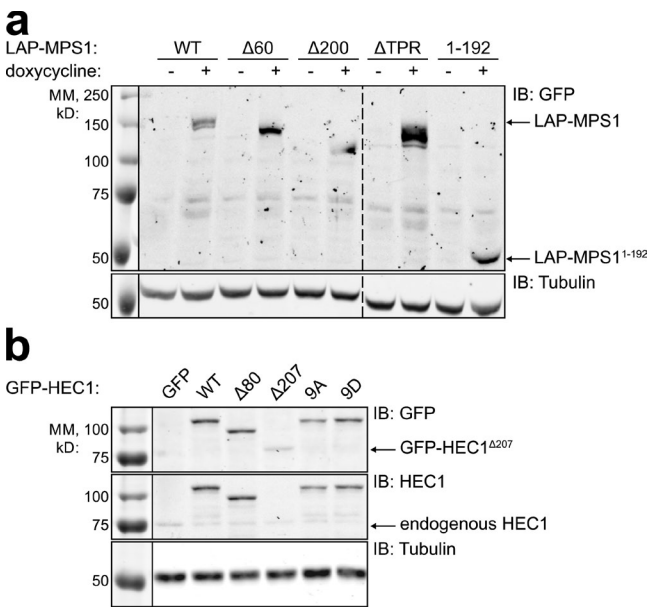

Figure S3. **HeLa-FRT LAP-MPS1 and HeLa Flp-in GFP-HEC1 cell lines.** (a) Immunoblot of whole-cell lysates from mitotic HeLaK FRT TetR LAP-MPS1 cell lines that were induced (+ doxycycline) to express the indicated LAP-MPS1 proteins. Dotted line indicates excision of lanes. (b) Immunoblot of whole-cell lysates from mitotic HeLa Flp-in GFP-HEC1 cell lines that were induced to express the indicated GFP-HEC1 proteins. Boxes on left show molecular mass standard. IB, immunoblot; MM, molecular mass; WT, wild type.

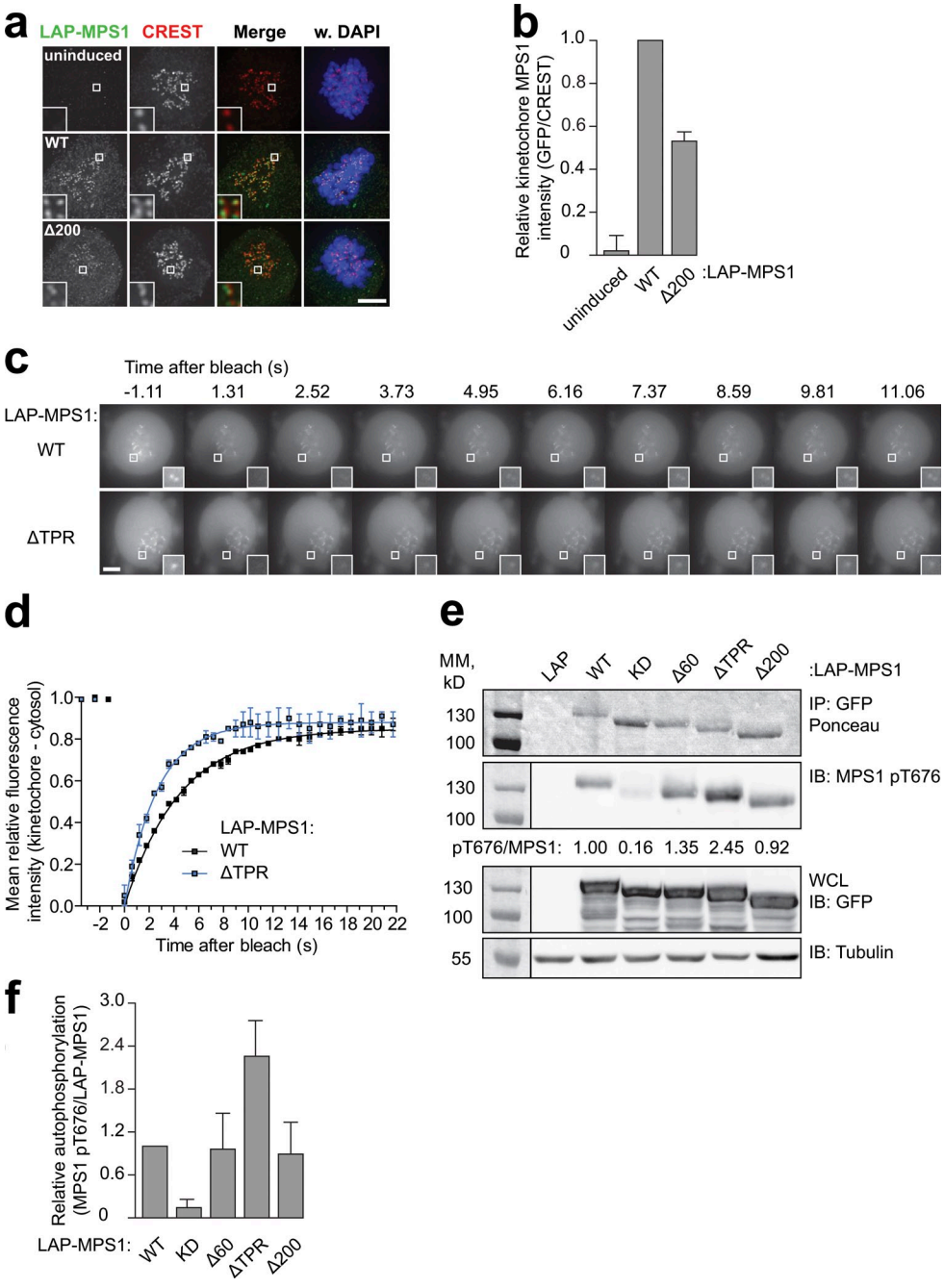

Figure S4. **N-terminal MPS1 mutants retain kinase activity and display normal residence time at unattached kinetochores.** (a and b) Representative images (a) and quantification (b) of immunolocalization of the indicated LAP-MPS1 proteins (GFP) and centromeres (CREST) in HeLaK FRT TetR cells treated with nocodazole, 0.5 µM reversine, and MG132. DNA (DAPI) is shown in blue. Insets show magnifications of the boxed regions. Graph in b shows total kinetochore intensities (±SEM) of LAP-MPS1 relative to centromeres. Data are from ≥19 cells from two experiments. Ratios for LAP-MPS1^{WT}–expressing cells are set to 1. (c and d) Fluorescence recovery after photobleaching of LAP-MPS1^{WT}– or LAP-MPS1$^{\Delta TPR}$–expressing Flp-in HeLa cells that were treated with nocodazole, MG132, and 500 nM reversine. Areas centered on single kinetochore pairs were bleached at $t = 0$ s. Insets show magnifications of the boxed regions. Graph in d shows the mean relative fluorescence intensities versus time (seconds) of the kinetochore regions from which intensities of neighboring cytosolic regions were subtracted (±SEM). Data points have been fitted, yielding the curves shown (solid lines). LAP-MPS1^{WT} recovered with a $t_{1/2}$ of 3.0 s and a signal recovery of 0.85. LAP-MPS1$^{\Delta TPR}$ recovered with a $t_{1/2}$ of 1.8 s and a signal recovery of 0.88. Data are from three experiments and a total of ≥34 cells per condition. (e and f) Autophosphorylation assay of the indicated LAP-MPS1 proteins. (top) MPS1 pT676 immunoblot (IB) and total protein levels are shown for immunopurified (IP) LAP-MPS1 from mitotic HEK 293T cells; band intensity of MPS1 pT676/total protein relative to LAP-MPS1^{WT} is indicated. (bottom) LAP-MPS1 (GFP) and tubulin immunoblots are shown for cell lysates. Graph in f shows relative MPS1 pT676 intensity (±SD) relative to total protein. Data are from three experiments. Ratios for LAP-MPS1^{WT} are set to 1. Boxes on left show molecular mass standard. Bars, 5 µm. MM, molecular mass; WT, wild type; KD, kinase dead; WCL, whole-cell lysate.

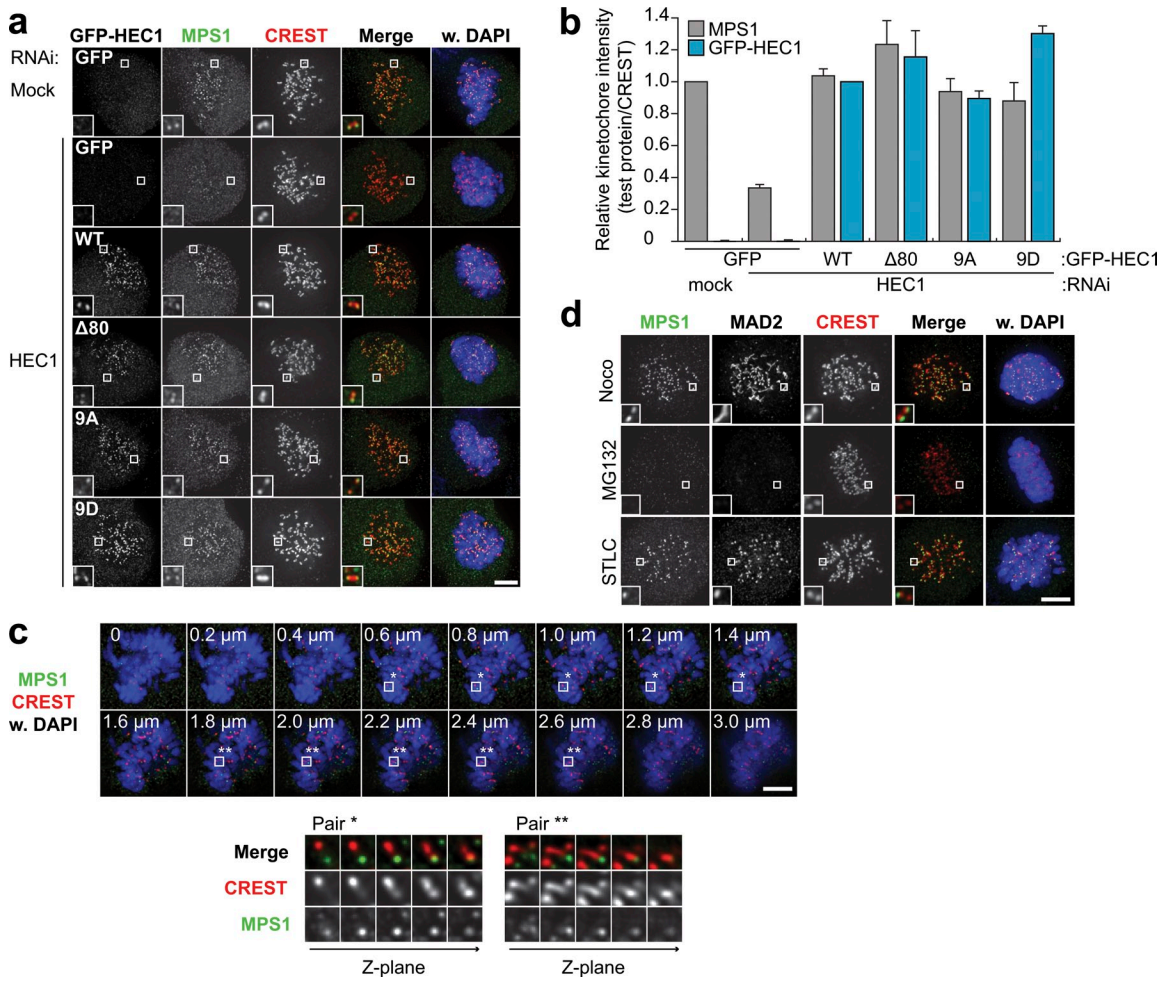

Figure S5. **MPS1 localization is dependent on kinetochore–microtubule attachment status but independent of Aurora B phosphorylation of the HEC1 tail.** (a and b) Representative images (a) and quantification (b) of immunolocalization of the indicated GFP-HEC1 proteins and centromeres (CREST) in HeLa Flp-in cells transfected with mock or HEC1 siRNAs and treated with nocodazole and reversine (0.5 μM). DNA (DAPI) is shown in blue. Insets show magnifications of the box regions. Graph in b shows total kinetochore intensities (±SEM) of MPS1 and GFP-HEC1 relative to centromeres. Data are from ≥41 cells from two experiments. Ratios for mock RNAi–treated cells are set to 1. Ratios of MPS1 localization are set to 1 for mock RNAi–treated cells or, for GFP-HEC1 localization, are set to 1 for GFP-HEC1^{WT}–expressing cells. (c) Immunolocalization of MPS1 and centromeres (CREST) in an unperturbed prometaphase HeLa cell. Images show individual z planes at a 0.2-μm interval, as indicated. Asterisks indicate representative sister kinetochores pairs that are shown in the magnifications below. DNA (DAPI) is shown in blue. (d) Immunolocalization of MPS1 and centromeres (CREST) in HeLa cells that were treated with nocodazole (Noco), MG132, or *S*-trityl-L-cysteine (STLC) for 30 min. DNA (DAPI) is shown in blue. Insets show magnifications of the boxed regions. Bars, 5 μm. WT, wild type.

A ZIP file is provided that shows (a) background_select: ImageJ macro that selects and thresholds all chromosome areas using the DAPI channel; (b) kinetochore_select: ImageJ macro that selects and thresholds all centromere areas using the CREST channel and subsequently selects an area encompassing the chromosomes, excluding centromere areas; and (c) kinetochore_measure: ImageJ macro that measures mean fluorescence intensities of the chromosome area, excluding centromeres and of the centromere area.